Cent. Eur. J. Geosci. • 2(4) • 2010 • 433-440
DOI: 10.2478/v10085-010-0010-y

VERSITA

Central European Journal of **Geosciences**

Thermoluminescence of quartz from Shihu gold deposit, western Hebei province, China: some implications for gold exploration

Research Article

Ye Cao [123*], Shengrong Li [12], Meijuan Yao [123], Huafeng Zhang[12]

1 *State Key Laboratory of geological processes and mineral resources, China University of Geosciences, Beijing 100083, China*

2 *School of Earth Science and Resources, China University of Geosciences, Beijing 100083, China*

3 *Department of Earth Sciences, Laurentian University, Sudbury,P3E2C6, Canada*

Received 19 February 2010; accepted 13 May 2010

Abstract: Thermoluminescence (TL) of monomineralic separates have been widely used in various geosciences fields in order to trace the thermal history and aid in prospecting for gold deposits. Quartz is a ubiquitous mineral in the Shihu gold deposit, which is situated in the northern part of the Taihang orogenic belt in the North China craton (NCC). The deposit is hosted by ductile-brittle faults within an Archean metamorphic core complex of the Fuping Group. This deposit is characterized by gold-bearing quartz-polymetallic sulfides and quartz veins. New TL results have been obtained for quartz, in which four type-TL glow curves were identified. The gold-bearing quartz present type III glow curves that consist of two peak glow curves at the middle and high peak temperatures with the similar TL intensity. In addition, the cross-sections of peak temperatures and TL intensity highlight the valuable area where the Au-bearing quartz present weak TL intensity and low-middle peak temperatures. Our results significantly enhance the usefulness of quartz in metallogenic studies of the North China craton and as an indicator mineral in mineral exploration of the Taihang Mountain region.

Keywords: thermoluminescence • quartz • Shihu gold deposit • prospecting

1. Introduction

A ubiquitous silicate mineral in gold deposits, quartz is vulnerable to dissolution and reprecipitation in hydrothermal systems. It is therefore a good material for recording and storing the evolution of hydrothermal metallogenic systems, especially compared to other minerals that may be much more altered. Quartz commonly shows intense luminescence under the appropriate stimulation. Thermoluminescence (TL) is the emission of visible light by heating [1]. TL results from a thermal activation of electrons trapped by the lattice defects of a crystal [2]. Therefore, TL requires chemical or physical defects in a mineral and the trapping of electrons by these defects. The number and

*E-mail: cykaiyang@yahoo.com.cn

the features of electron traps – or the glow curve shapes – are chiefly dependent on crystallization or recrystallization conditions. Radiation or thermal effects caused by high temperature events can also lead to a displacement process of atoms. However, these last effects are unusual in the cases studied for gold exploration [3]. Attempts to use TL as an exploration tool began in the USA and in Canada with the studies of reference [4]. Charlet et al. (1987) [5] has summarized the use of TL for mineral exploration. TL glow curves are often complex, which provide a good way to discriminate between quartz of various origins (e.g barren quartz and mineralization quartz). In general, though TL intensity of quartz is often very low, the luminescence properties of quartz have been used for prospecting in many gold deposits in China over the past decade [6–8]. The objectives of the present study are to determine peak temperature, intensity of TL of quartz from different ore-forming stages, and then evaluate its usefulness for prospecting.

2. Regional and district geological setting

The North China craton (NNC, also known as the Sino-Korean craton) with basement rocks as old as 3.8 Ga [9] (Figure 1a) is located in the eastern part of the Euro-Asian continent, bounded to the north by the southern margin of Central Asian Orogenic Belt (CAOB) and to the south by the Dabie-Sulu ultra-high pressure (UHP) belt that formed during a process of Triassic collision between the Yangtze Block and the NCC [10]. The Taihang Mountain, part of the NE-SW trending giant gravity lineament (NSGL) (Figure 1b) was identified based on geophysical data [11]. According to recent work, the Taihang Mountain is a special geomorphological-tectonic unit within the North China craton which separates the Ordos cratonic block in the west and the North China semicircular rift basin in the east [12]. The region to the west of the NSGL shows large negative Bouguer gravity anomalies and is underlain by a thick (150-220 km) lithospheric mantle; the region to the east of the NSGL, however, shows weakly negative to positive Bouguer gravity anomalies and high heat flow and is underlain by a relatively thin lithosphere (60-120 km) [13]. Extensive Mesozoic magmatism, together with the development of large-scale sedimentary basins, occurs mainly in the region east of the NSGL, in contrast to the minor magmatism in the region west of the gravity lineament.

The base of Taihang Mountain mainly consists of Archean tonalite-trondhjemite-granodiorite (TTG) gneiss, which are unconformably overlain by thick sequences of Meso- to Neo-Proterozoic clastic and chemical sedimentary rocks, suggesting that the craton was stabilized by the Paleo-Proterozoic. The craton was stable until the late Triassic when widespread volcanism (predominantly basaltic, andesitic and dacitic rocks, with minor rhyolites) and intrusion of dominantly intermediate to felsic plutons occurred, accompanied by large-scale basin formation. The Mesozoic magmatism continued intermittently until the late Cretaceous, and resulted in the NE-trending magmatic belts in East China [14]. Voluminous Mesozoic intrusions occur in the orogen, with rock types dominated by monzonites, monzogranites and related mafic rocks. Chen, et al. (2008) [15] reported SHRIMP zircon U-Pb ages of 127±3 Ma and 129±3 Ma for a quartz monzonite pluton and a monzonite pluton in the orogen, respectively. A slightly older age of 138±2 Ma was also reported by Chen, et al., (2005) [16] for a mafic pluton from the orogen.

The Shihu gold mining district covers 4.1229 km^2, centered on geographic coordinates 114°03′15″E–114°04′21″E and 38°38′04″N—38°40′19″N. The deposit is a typical Shihu-type gold system with quartz-sulfide veinlets (Figure 1c). The wall rocks consist of metamorphosed Precambrian sequences, including tectonically flattened and foliated 2.5~2.4 Ga TTG gneisses, ~2.5 Ga Wanzi paragneisses mainly derived from aluminous schist and gneisses with minor amounts of calc-silicate rocks, marbles and amphibolites, and ~2.0 Ga Nanying granitic gneisses, commonly containing the TTG as xenoliths, mainly derived form monzogranitic and syenogranitic varieties [17, 18]. All of which are metamorphosed to upper-amphibolite to granulite facies. The Mapeng granitoid batholith, with a total exposed area of about 64.5 km^2, is the most impotant intrusion in the Shihu gold mine area. The batholith intruded the Archean Fuping complex and is composed mainly of medium- to coarse grained massive granites. Small mafic enclaves (5-15 cm long) that have sharp contacts with the host granite are locally present. In addition, there is a NE- striking swarm of diorite and quartz diorite porphyrite dikes that intrude into the Archean Fuping complex, broadly parallel to the gold-bearing quartz vines.

The Shihu gold deposit is restricted by NNE-NE trending faults. More than 50 quartz veins have been identified in the deposit, which trend N/S and dip west or east. These veins are generally 2-5 m in width and hundreds of meters in length. The main lode is approximately 3200 m long and 2-5 m wide (locally up to 10 m), and has an average gold grade of 5.88 g t^{-1} with a maximum grade of 100 g t^{-1} [19] (Figure 1d). In terms of paragenetic sequences, these gold-bearing veins can be divided into three types: (1) pyrite phyllic veins; (2) disseminated pyritization veins; and (3) polymetallic sulfide veins. Alteration around the veins comprises mainly K-feldspathization, pyrite phyllic

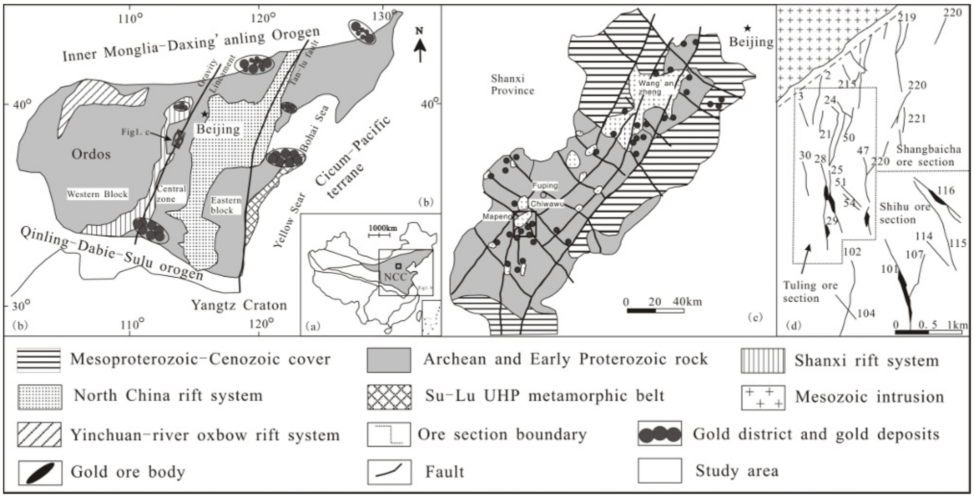

Figure 1. Generalized map of the Shihu gold deposit, western Hebei province (Modified by references [20–23]).

alteration, silicification and intensive polymetallic sulfide as well as lesser carbonatization, sericitization, kaolinization, and chloritization. Among the alteration assemblages, the intensive polymetallic sulfide and silicification are most closely associated with gold mineralization. According to ore textures, structures and mineral assemblages, ore-forming processes are divided into four stages: a pyrite phyllic stage (1), A smoky gray Au-bearing quartz, fine-grained pyrite stage (2), A Au-bearing polymetallic sulfide-quartz stage (3), A quartz-carbonate stage (4). The stage 3 and stage 4 are the main ore-forming stages and the superposition of these two stages form bonanza zones. Ore structures commonly commonly include automorphic granular structures, poikilitic structures and immiscible structures. Ore minerals are predominantly pyrite, galena, sphalerite, chalcopyrite and magnetite, with minor pyrrhotite, bornite and native ruthenium [24]. Gold minerals are predominately native gold and electrum with trace amounts of kustelite (Figure 2). The shape of gold minerals are dominated by spherulitic, flake-like and dendritic. Quartz, K-feldspar, plagioclase, carbonate, biotite, sericite and chlorite constitute characteristic gangue mineral assemblage for both ore types.

3. Samples and Method

Seventy-one hydrothermal quartz samples from the Shihu lode gold deposit were selected from underground mining area at different levels: 560 m, 400 m, 360 m, 300 m, 260 m, 220 m, and 180 m. For quartz, TL intensity is often very low, so it is necessary to use an apparatus with a detection system sensitive to low light. Therefore, we used a new

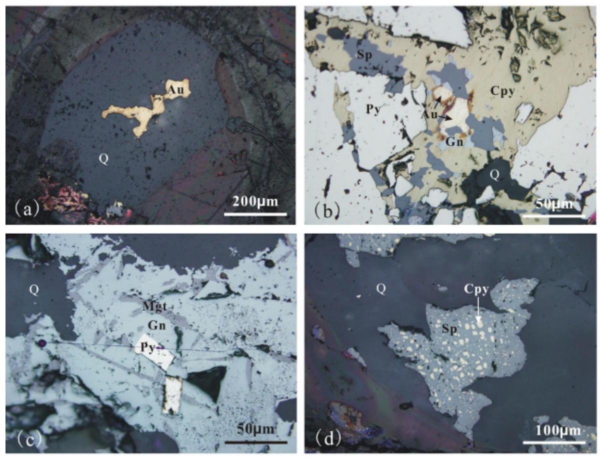

Figure 2. Ore mineral assemblage and structure of the Shihu gold deposit in western Hebei province.
Au=gold; Q=quartz; Gn=galena; Cpy=chalcopyrite; Py=pyrite; Mgt=magnetite; Sp=sphalerite

model FJ-427A1 TL apparatus developed by Beijing Nuclear Instrument Factory. All experiments were conducted in the Laboratory of Genetic Mineralogy, China University of Geosciences, Beijing. Initially, the samples were crushed to a grain size of approximately 200 to 300 μm using a carefully pre-cleaned agate mortar and pestle. About 100 mg of pure quartz grains without visible impurities were hand-picked using a binocular microscope. The calcite and dolomite impurities on the surface were readily removed from the sample after 24 hours of 10% HCl etching. Thereafter, all samples were repeatedly washed with diluted HNO_3 and ultrapure water, and finally evaporated to dryness at 50°C. The pure quartz was stored in acid cleaned glass tubes. Quartz aliquots of about 2 mg were heated in the TL apparatus for 470 seconds at a linear heating rate of 1°C s^{-1}.

4. Results

The TL results are summarized in the following Table 1. Double-peak glow curves were observed for 23 samples (32% of the total) and single-peak curves for the rest. No glow curves with more than 2 peaks were observed.

5. Discussion

5.1. Analysis of TL curves

A plot of light emission versus temperature is called a "glow curve", and often shows several glow peaks. The main TL properties are obtained from the glow curves by plotting the light intensity of a mineral powder against the temperature. In mineral exploration, different types of quartz can be distinguished by using the number, temperatures and relative intensities of the glow peaks. The glow peaks may be characterized by a statistical study of the distribution of the light emissions temperatures and, after that, by a calculation of the mean value, the statistical dispersion and the frequency of the appearance of the glow peaks defined in this way. For the Shihu gold deposit, four different types of glow peak have been identified. Examples of Types I-IV are shown in Figure 3.

Using cross-cutting relationships of veins in the mine, the ore-forming processes of the Shihu gold deposit can be divided into four metallogenic stages: a pyrite-quartz stage, a quartz-pyrite stage, a quartz-polymetallic sulfide stage and a quartz-carbonate stage, in sequence from early to late. Petrographic textures displayed in Figure 3 shows that the type I curve is associated with stage 1 quartz, characterized by milky white quartz without sulfide; the type II curve is typical of quartz associated with the gold mineralization of quartz-pyrite stage 2, in which pyrites are the main sulfide in the quartz veins; the type III curve is typical of smokey quartz of the quartz-polymetallic stage 3; and the type IV curve is mainly found in the quartz associated with carbonatization and ferrocalcite parageneses of stage 4.

The number of electrons trapped, (which gives the TL intensity) is dependent on various factors [3]:

- TL sensitivity with respect to to crystallization or recrystallization conditions.
- Radioactivity: this increases the number of electrons trapped but with a saturation level related to the nature of the mineral and its radioactive and thermal history.
- Thermal or photodesexcitation effects which decrease the number of trapped electrons. Thus, geothermal effects, sunlight and paleoclimatological conditions can modify the filling rate of the traps.

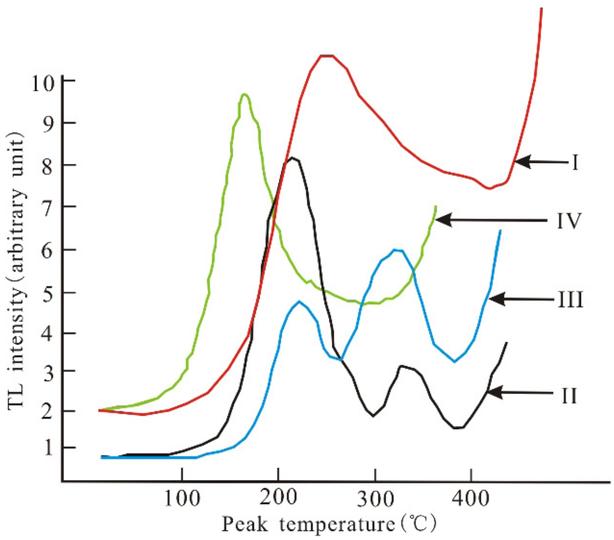

Figure 3. TL glow curves of quartz samples consist of four metallogenic stages in the Shihu gold deposit, western Hebei province.

The quartz in stage 1 is characterized by single-peak glow curves at the peak temperature ranging from 200 to 260°C with the large scope of TL intensity ranging from 1000 to 10000 arbitrary units. The quartz in stage 2 are typical of two-peak glow curves corresponding to middle-low and high peak temperature with conspicuous TL intensity exemplified by the sample collected at 11 exploration line at the 180 m level. It shows a low-temperature peak at 192°C of 8470 arbitrary units and a weaker high-T peak of 1305 arbitrary units at 329°C. Collected from high grade Au-bearing quartz veins occurring nearby the quartz diorite porphyry dykes, the sample was transformed by ore-forming fluid suggested by the typical glows curves at stage 2. The quartz in stage 3 feature two-peak glow curves corresponding to middle and high peak temperatures with similar TL intensity of about 3000 arbitrary units. The glow curve for stage 4 quartz is typified by that of the sample from the 29 exploration line at the 220 m level, which has a narrow peak at temperatures below 200°C and of maximum intensity of 10000 arbitrary units. This glow curve indicates the samples of quartz formed

Table 1. Results of quartz thermoluminescence from the Shihu gold deposit, western Hebei.

Level (m)	Exploration line	Peak temperature low	medium	high	TL Intensity (arbitrary units)	Level (m)	Exploration line	Peak temperature low	medium	high	TL Intensity (arbitrary units)
180	5			267	2657	260	27			272	740
180	7			255	18135	260	29		251	293	831/1935
180	9		220		8391	260	31		241		6780
180	11	192		329	8470/1305	300	9			262	5552
180	13	192	243		1780/2334	300	11		218		4190
180	15		278	315	631/846	300	13		249		1557
180	15.5		255		1780	300	15		232		1150
180	17		236		1662	300	17		259		595
180	19			269	1630	300	21		234	302	1807/975
180	19.5		236		4675	300	23		257		1474
180	21		242	294	1238/1696	300	25		262		2010
180	23		206		4466	300	29		251	262	1646/1813
180	25		252		1433	400	0		257		2319
180	29.5			273	2769	400	1		224		33452
180	31.5		232		5828	400	3		237	293	1232/1382
220	3		227		1601	400	5			290	866
220	5			268	820	400	7		241		4266
220	7		220		3474	400	9		237		1340
220	9		246		1190	400	11		244		3200
220	15		236		2335	400	13		228		2807
220	17		237	293	4054/1871	400	15		225	261	2612/2847
220	19			259	519	400	19		230		11537
220	23		224		5151	400	21		231	301	547/1527
220	25		222		2183	400	23			290	3316
220	29	168			11789	400	25		238	304	1991/3154
220	31		212		4816	480	11		224	269	1176/1276
260	5	183			5739	480	13		230	259	785/769
260	7		245		1278	480	15		231	262	7479/7059
260	9	184			4088	480	23			263	2242
260	11		236	304	1717/1086	560	5		208	235	6519/5585
260	17		245		905	560	7		228	267	1997/1636
260	19			266	592	560	7.5		218	266	1160/987
260	21		251	314	2746/1271	560	9		223		3412
260	21.5		252	288	919/1149	560	11			263	791
260	23		251	314	2746/1271	560	13		235	307	1138/1633
260	25		245		2228						

shallowly and captured a larger number of electrons in electron traps of weaker energy levels [25].

5.2. Implications for gold exploration

Seen together, the gradual increase in TL peak temperatures coincides with decreasing TL intensities (R^2=0.49) (Figure 4), suggesting a negative correlation between the number of trapped electrons and their depth of trapped energy levels [26]. In general, quartz crystals constantly received and accumulated the amount of external radiation. Electrons trapped in deep energy traps require high temperatures demanding excitation sufficient to escape from the trap [27, 28], whereas electrons in shallow traps can escape even at lower temperatures. Therefore, older quartz shows relatively stronger high-temperature glow peaks, while later stage quartz shows enhanced low-temperature peaks [29]. Consistent with field observations, the type I and type IV glow curves of Figure 3 correspond to the earliest and latest quartz. However, the peak shapes and peak numbers are affected by the number and types of structural impurities in the quartz. The more impurities the quartz has, the more complicated the glow curves become [30].

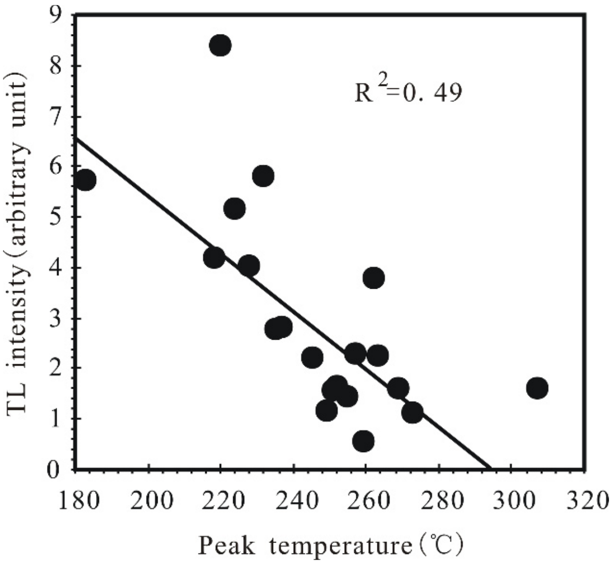

Figure 4. Correlations between peak temperatures and TL intensities of the quartz samples from the Shihu gold deposit, western Hebei province.

TL characteristics show conspicuous regional trends in their peak temperatures and TL intensities throughout the studied area. Glow curve characteristics can provide some geological context in which to judge the properties of the Au-bearing quartz veins [31]. The type III glow curves, as an indicator of economic minerals, can be applied to prospecting and surface exploration work [6, 7]. Cross-sectional maps of peak temperatures and TL intensity were compared to those of gold grade (Figure 5 and 6). These projections indicate that the TL intensity at 2000-6000 arbitrary units of quartz corresponds to high-grade quartz veins, while weaker or stronger TL indicates barren quartz. Furthermore, low-to-medium peak temperatures (< 300°C) also indicate a high gold grade. For example, the peak temperature is smaller than 200°C at 29 and 31 exploration lines at the 210 m level, between 250°C and 290°C at 19 exploration lines at the 350 m level, and at the 3 exploration line at the 480 m level. It inferred that a possible area for future prospecting is the area northward of the 3 exploration line at the 200 m level, and between the 19 and 31 exploration lines in deep areas, however, there may be a barren area between the 7 and 15 exploration lines in the deep areas.

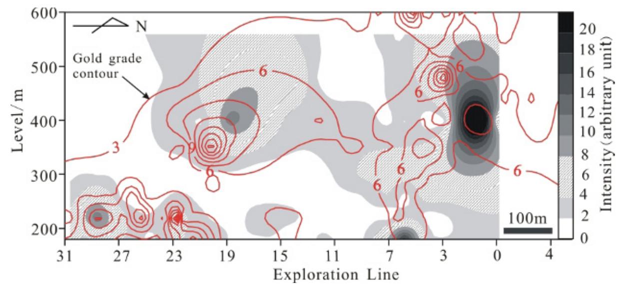

Figure 5. Comparison of cross-sectional maps between intensities and the gold grade of quartz samples from the Shihu gold deposit, western Hebei province.

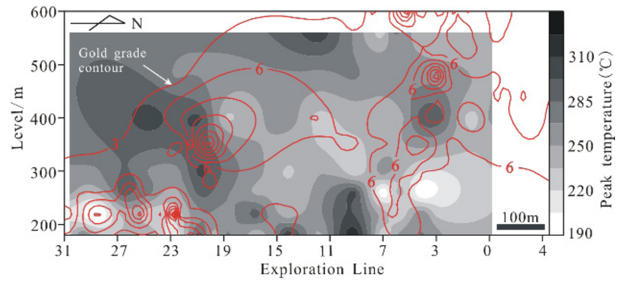

Figure 6. Comparison of cross-sectional maps between peak temperatures and the gold grade of quartz samples from the Shihu gold deposit, western Hebei province.

6. Conclusions

As an important method, mineralogical mapping is often applied to prospecting. Quartz TL is an easy and low-cost method as applied to the assessment of exploration prospects in the Shihu gold deposit. New results have been obtained for quartz and the results are promising. Through the comparison of TL glow curves, peak temperature, TL intensity and gold grade, it is shown that the gold-bearing quartz correlates with type III glow curves, with middle and high temperature glow peaks of similar TL intensity. Moreover, the cross-sectional maps of peak temperatures and TL intensity highlight areas of economic deposits, in which the Au-bearing quartz present weak TL intensity and low-middle peak temperature. Recognition of quartz related to mineralized rocks can provide a rapid and cost-effective way to find mineralization by more detailed sampling.

Acknowledgements

Funded by National Natural Science Foundation of China Major Research Plan Key Support Project (Grant No. 90914002), and the 111 Project under the Ministry of Education and the State Administration of Foreign Experts Affairs, China (Grant No. B07011). Thanks to special funds provided by the National Crisis Resources Prospecting Mining project management office. Thanks to Wang Wenxue secretary of Shijiazhuang Comprehensive Geological Brigade and other colleagues of the Shihu Gold Deposit Company for their enthusiastic help with field work.

References

[1] Chen R., McKeever S.W.S., Theory of thermoluminescence and related phenomena, World Scientific Press, Singapore, 1997

[2] Cao Y., Li S.R., Yang L.F., Tong J.G., Gao Y.H., Luo J.Y., Thermoluminescence characteristics of otoliths of wild carps (cyprinoid) in the Baiyangdian Lake and Miyun Reservoir, Acta Petrol. Mineral. (in Chinese), 2006, 25, 449-454

[3] Charlet J.M., Quinif Y., Quartz thermoluminescence (TL) in gold exploration; some applications, Mineral. Deposita, 1990, 25(Suppl), 13-20

[4] McDougall D.J., Thermoluminescence of rocks as prospecting tool. Equipment and methods. Trans. Can Inst. Min. Metal., 1965, 68, 247-252

[5] Van Moort J.C., Russel D.W., Electron spin resonance of auriferous and barren quartz at Bea consfield, Northern Tasmania, J. Geochem. Exploration, 1987, 2, 1-11

[6] Chen G.Y., Sun D.S., Yin H.A., Genetic mineralogy and prospecting mineralogy (in Chinese). Chong Qing Press, Chong Qing, 1984

[7] Chen G.Y., Sun D.S., Shao W., Atlas of Mineralogical Mapping in East Jiao dong Gold Province, Geological Publishing House, Beijing, 1996

[8] Li S.R., Chen G.Y., Shao W., Sun D.S., Genetic mineralogy of Rushan gold deposit in Jiaodong peninsula (in Chinese). Geological Publishing House, Beijing, 1996

[9] Liu R.X., Geochronology and Geochemistry of the Cenozoic Volcanic Rocks in China (in Chinese). Seismic Press, Beijing, 1992

[10] Li S.G., Xiao Y.L., Liu D.L., Chen Y.Z., Ge N.J., Zhang Z.Q., Sun, S.S., Collision of the North China and Yangtze Blocks and formation of coecite-bearing eclogites: timing and processes, Chemical Geology, 1993b, 109, 98-111

[11] Ma X.Y., Liu G., Su J., The structure and dynamics of the continental lithosphere in north-northeast China, Annals of Geophysics, 1984, 2, 611-620

[12] Menzies M., Xu Y.G., Zhang H.F., Intetration of geology, geophysics and geochemistry: A key to understanding the North China Craton, Lithos, 2007, 96, 1-21

[13] Deng J.F., Zhao H.L., Mo X.X., Continental Roots-Plume Tectonics of China (in Chinese). Geological Publication House, Beijing, 1996

[14] Deng J.F., Wei W.B., The three dimensional structure of lithosphere and its evolution in north China (in Chinese). Geological Publication House, Beijing, 2007

[15] Chen B., Tian W., Jahn B.M., Chen Z.C., Zircon SHRIMP U-Pb ages and in-situ Hf isotopic analysis for the Mesozoic intrusions in South Taihang, North China craton: Evidence for hybridization between mantle-derived magmas and crustal components, Lithos, 2008, 102, 118-137

[16] Chen B., Tian W., Zhai M.G., Arakawa Y., Zircon U-Pb geochronology and geochemistry of Mesozoic magmatism in the Taihang Mountains and other places of the North China Craton, with implications for petrogenesis and geodynamic setting, Acta Petrol. Sin. (in Chinese), 2005, 21, 13-24

[17] Liu S.W., Study on fluid-rock equilibrium systems of Fuping gneiss complex, Taihang Mountains, Science in China, Ser D, 1997, 40, 239-251

[18] Liu S.W., Pan Y.M., Xie Q.L., Zhang J., Li, Q.G., Archean geodynamics in the Central Zone, North China Craton: constraints from geochemistry of two contrasting series of granitoids in the Fuping and Wutai complexes, Precambrian Res., 2004, 130, 229-243

[19] Wang J.S., Tian B.L., Li C.L., Geological exploration report on the middle section of Tuling-Shihu gold mining area, 520 Team of first Geological Exploration Bureau of Ministry of Metallurgical Industry, Nov., 1990

[20] Liu W., Dai T.G., Fu W.J., Sun S.D., Hu B., Ore occurrence regularity and prospecting of Shihu gold deposit in the western Heibei province, Geology and prospecting (in Chinese), 2007, 43, 25-33

[21] Liu W., Dai T.G., Fu W.J., Sun S.D., Hu B., Characteristics of ore-forming fluids of the Shihu gold deposit, western Hebei (in Chinese), Geol. in China, 2007, 34, 335-340

[22] Niu S.Y., Chen L., Xu C.S., Crustal evolution and metallogenic regularity in the Taihang mountains (in Chinese). Earthquake publishing house, Beijing, 1994

[23] Tang Y.J., Zhang H.F., Ying J.F., Zhang J., Source characteristics and temporal-spatial evolution of Mesozoic and Cenozoic basaltic magmatism in the Taihang Mountains (in Chin.), Acta Petrol. Sin., 2006, 22, 1657-1664

[24] Peng Q.M., Xu H., The discovery of native ruthenium in Nuanquanzi and Tuling-Shihu gold deposits: Implications for Source of Gold, Chinese J. Geochem.,

1994, 13, 123-131

[25] Benoit P.H., Hartmetz C.P., Batchelor J.D., Symes S.J.K., Sears D.W.G., The induced thermoluminescence and thermal history of plagioclase feldspars, Am. Mineral., 2001, 86, 780-789

[26] Chen R., Kinetics of Thermoluminescence Glow Peaks. Cambridge University Press, Cambridge, 1984

[27] Miallier D., Gibert F., Fain J., Pilleyre Th., Sanzelle S., Fluid inclusions in quartz: interference with thermoluminescence and its application to dating, Quaternary Sci. Rev., 2001, 20, 901-905.

[28] Rasheedy M.S., A new evaluation technique for analyzing the thermoluminescence glow curve and calculating the trap parameters. Thermochim. Acta, 2005, 429, 143-147

[29] Wang K.Y., The application of thermoluminescence of quartz to evaluate the auriferous feature of mineralized veins in Qiangma gold deposit (in Chinese). Geology and Prospecting, 2000, 36, 37-39

[30] Huang F., Wang J.G., Zheng C., Zhao C.F., The characteristics of composition and thermoluminescence of quartz in Shaoguoyingzi gold desposit (in Chinese). Journal of precious metallic geology, 1998, 7, 43-47

[31] Tan K.X., Gong G.L., Thermoluminescence characteristics of sand-shale copper deposits and their implication for ore Genesis (in Chinese). Acta Mineral. Sin., 1999, 19, 183-188